Available online at www.sciencedirect.com
SCIENCE DIRECT®
PERGAMON
International Journal of Heat and Mass Transfer 46 (2003) 4613–4627
International Journal of HEAT and MASS TRANSFER
www.elsevier.com/locate/ijhmt

Calcium carbonate scaling in a plate heat exchanger in the presence of particles

N. Andritsos *, A.J. Karabelas

Department of Chemical Engineering, Chemical Process Engineering Research Institute/CERTH, Aristotle University of Thessaloniki, P.O. Box 361, GR 57001, Thermi-Thessaloniki, Greece

Received 27 August 2002; received in revised form 3 June 2003

Abstract

Scale formation of $CaCO_3$ in a plate heat exchanger is investigated in the presence of various types of added particles under isothermal conditions. The parameters examined include the degree of supersaturation, the type of particles, the flow velocity, the particle concentration and the direction of flow inside the heat exchanger. The key result of this work is the strong synergistic effect of fine aragonite particles on the deposition rate and the morphology of the deposits. On the contrary, the presence of fine titanium oxide and of relatively large calcite particles does not seem to affect the main scaling characteristics of $CaCO_3$.

1. Introduction

Fouling, the accumulation of undesirable deposits on industrial equipment surfaces, is a complex phenomenon with severe economic consequences, affecting a wide range of industrial processes. Research on fouling has made significant progress over the past 30 years in understanding the governing mechanisms of the fouling process, although several aspects of this phenomenon have not been elucidated yet, and predictive tools are inadequate. The deposits may consist of crystalline, particulate and biological matter or can be products of chemical reactions or corrosion. In most cases more than one type of matter is present in the deposits. It is generally accepted that five main fouling categories exist, depending on the prevailing process [1,2]; i.e., crystallization (or precipitation), particulate, chemical reaction, corrosion and biological fouling.

Precipitation fouling usually refers to the formation of a solid layer on equipment surfaces arising from the direct crystallization on the wall of dissolved inorganic salts. Fluid supersaturation is brought about through temperature or pH changes, or through mixing of incompatible water streams. The term "scaling" often refers to the formation of deposits of inverse-solubility salts ($CaCO_3$, $CaSO_4$, $Ca_3(PO_4)_2$ etc.), although it generally denotes the hard, and adherent deposits due to inorganic constituents of water [3].

Suspended solids are almost always present in industrial processes, such as cooling water systems. They can accumulate on equipment surfaces forming in general, "loose" deposits. Moreover, their presence can affect the formation of crystalline deposits in various ways. There is a common belief that the presence of particulates renders the scale deposits "softer" and less coherent. On the other hand, several investigators report that the presence of particles tends to increase significantly the deposition rate of $CaCO_3$ [4,5]. Calcium carbonate is by far the most common scale compound, forming tenacious layers in several industrial systems, including cooling water circuits, potable water supply lines, desalination units, and petroleum and gas production systems [3]. The main causes of calcium carbonate deposition are CO_2 loss from the solution (resulting in pH increase) and the temperature or salt concentration increase. The calcium carbonate solubility decreases with increasing pH and temperature and increases with increasing partial

* Corresponding author. Present address: Department of Mechanical and Industrial Engineering, University of Thessaly, 383 34 Volos, Greece. Fax: +30-231-049-8189.
E-mail address: andritso@cperi.certh.gr (N. Andritsos).

0017-9310/$ - see front matter © 2003 Elsevier Ltd. All rights reserved.
doi:10.1016/S0017-9310(03)00308-9

pressure of carbon dioxide. Three calcium carbonate polymorphic modifications are commonly encountered in deposits, i.e. calcite, aragonite and vaterite. Formation of a certain modification is influenced by the solution temperature, the level of supersaturation and the presence of foreign ions or particles. Although calcium carbonate is possibly the most extensively researched scaling compound, no systematic study is available in the literature on the effect of particle presence on $CaCO_3$ scale formation. In this work, a research effort involving three types of commercial particles has been undertaken to investigate the influence of suspended matter on the $CaCO_3$ scale formation inside a plate heat exchanger (PHE), as well as in a tubular test section, under isothermal conditions. The choice of isothermal conditions was made to simplify the complicated process of scaling. Furthermore, due to the need to carry out a large number of tests, this study deals essentially with the initial scaling conditions. Deposition of $CaCO_3$ (pure precipitation fouling) in pipe flow has already been studied in this laboratory [6,7]. PHEs are now widely used in various industrial sectors (process, food and pharmaceutical industry, air-conditioning, geothermal exploitation, etc.) and tend to gain broader acceptance compared to other exchanger types [8]. It is also believed that PHE are less prone to fouling than shell-and-tube exchangers for the same thermal duty [9].

2. Literature review

Several investigators in the past 30 years have reported cases where precipitation and particulate fouling proceed simultaneously. Moreover, the prevailing opinion is that the presence of particles in the system or the presence of more than one compound in the scale, can weaken its structure, thus facilitating the removal process and establishing asymptotic fouling [10,11]. In the literature, studies on the effect of particles on the scaling process deal mostly with the $CaCO_3$ and $CaSO_4$ systems.

The earliest work, known to the authors, on the effect of particles on $CaCO_3$ scaling is that of Lee and Knudsen [4], who present preliminary results obtained with suspended solids (in the form of river clay) at a concentration of 25 mg/l. It appears that the addition of these particles caused significant increase of the fouling factor in two out of three experimental runs. Similarly, Watkinson [5] reports that particulates (bulk precipitated $CaCO_3$ particles) increase the $CaCO_3$ scaling rate, even at concentrations as low as 6 mg/l, when compared with runs with an in-line filter. Furthermore, it appears that the scaling rate increases with increasing particle concentration.

Regarding the $CaSO_4$ scaling system, the first hint for a synergism between particles and scaling process was given by Hasson and Zahavi [12]. They observed a pronounced decrease of the scaling rate (by a factor of 3 or 4), when the recirculating fluid was filtered through a 20 μm filter. Bramson et al. [13] examined the effect of a relatively high $CaSO_4$ particle concentration on the scaling of a heated metal surface covered by a falling film. They too observed a substantial enhancement of $CaSO_4$ deposition rate in the presence of particles. The authors also reported that a loosely adherent $CaSO_4$ scale layer can become hard and tenacious through co-precipitation with $CaCO_3$.

In a recent review paper Hasson [14], among other aspects of precipitation fouling, summarises the work in the area till 1997. Stating that the role of particles in scale layer growth is quite complex, he notes that the available data in the $CaSO_4$ and $CaCO_3$ scaling systems suggest that the presence of particles can either enhance or reduce the scale deposition process. He further discusses four main parameters involved in the above effects:

(1) The nature of the scaling species (different phenomena occur with the $CaSO_4$ and $CaCO_3$ systems).
(2) Whether the scaling occurs in a sensible heating system or in an evaporative system (e.g. while the presence of $CaSO_4$ particles enhances fouling under sensible heat transfer conditions, the same particles reduce the wall crystallization process in an evaporative system).
(3) The flow velocity (low velocities enhance scale deposition).
(4) The nature of the particles (material similar or dissimilar to the scaling species; the latter seem to hinder the deposition process).

Bansal et al. [15] found that the presence of $CaSO_4$ particles (mostly generated from the detachment of crystalline deposits) enhances $CaSO_4$ scale formation in a PHE and showed that filtration of the recirculating solution resulted in significant reduction of fouling resistance, in agreement with previous work. They attributed the enhanced $CaSO_4$ scale formation rate to the fact that particulate deposits can create extra nucleation sites for crystal growth. On the other hand, "noncrystallizing" alumina particles were found to reduce the fouling resistance, which was attributed to higher removal rates associated with the reduction of deposit strength.

Recently, Andritsos and Karabelas [16] found that the presence of 40 mg/l of fine aragonite particles greatly increased the $CaCO_3$ deposition rates in tubes, especially at low fluid velocities. On the other hand, the same concentration of colloidal silica particles did not exhibit any effect on the precipitation characteristics. An interesting feature of the deposits formed in the presence of aragonite particles is their rippled appearance, with the

ripples arranged in the lateral direction, i.e. normal to the flow direction. Rippled deposits can be formed under both isothermal and heat transfer conditions with a variety of scaling species; an example of silica rippled deposits is reported by Gundmudsson and Bott [17]. These authors provide examples of rippled deposits and comment on possible mechanisms for their formation.

The synergism between calcium carbonate scaling and "dissimilar" particulate matter (silt and haematite) was also examined recently by McGarvey and Turner [18]. The presence of the above particles did not appear to affect the $CaCO_3$ scaling rate, although some crystal distortion was observed. However, the deposition rate of both types of particles was significantly increased (up to 715 times), following an induction period for calcite scaling. It was hypothesized that incorporation of particles into the growing calcite deposits provided a mechanism for particle attachment, that effectively bypassed the particle/stainless steel energy barrier. Most recently, Webb and Li [19] performed long-term combined precipitation and particulate fouling experiments in enhanced tubes using cooling tower water. The presence of particulates (silica, copper oxide and iron phosphate/silicate) resulted in "fluffy" deposits that could be easily removed by brushing, in contrast to the hard scale characteristics of pure precipitation fouling.

"Pure" precipitation fouling experiments were carried out in this laboratory under isothermal and heat transfer conditions [4,5,20]. It was found that the *initial deposition rate* increases sharply above a critical supersaturation ratio of approximately 7–8, remaining rather constant at higher ratios. Temperature and flow velocity have a marked effect on the deposition rate under these conditions, and an increase in both parameters results in higher deposition rates. At lower supersaturation ratios (<7) an "induction period" for the deposition is observed, which becomes longer as the supersaturation ratio decreases. It appears that the scale formation process is mass transport-controlled at supersaturation ratios greater than the critical one, while at lower ratios a surface reaction mechanism is operative. The dominant polymorph phase deposited is strongly dependent upon the solution temperature. Below 30 °C calcite is found to be the only polymorph formed. For supersaturation ratios greater that the critical one the flow apparently promotes columnar calcite formations. Above 35 °C dendritic formations of aragonite are mostly formed on the metal pipe surface.

It is well known that the presence of "seeds" induces bulk precipitation in a supersaturated solution e.g. [21–23]. Upon addition of the calcium carbonate seeds to a metastable $CaCO_3$ solution, precipitation is spontaneous, accompanied by a decrease of pH and total calcium concentration. House and Tutton [24] report that the addition of commercial calcite particles, to a solution supersaturated with respect to $CaCO_3$, tends to increase the precipitation rate with increasing particle concentration. The effect is more pronounced with calcite particles having a larger specific area. The situation is not as clear in cases where the seed crystals (pyrex glass seeds) are dissimilar in nature with respect to the precipitating system. House and Tutton report that the precipitation rate is also enhanced in the presence of a large concentration of pyrex particles (600–1800 mg/dm^3), but the increase is weaker compared to that of calcite seeds.

3. Experimental methods and analyses

A schematic diagram of the experimental set-up is shown in Fig. 1. Tap water is used in the experiments, its pH being adjusted by continuous addition of NaOH. Water is first passed through a filter for removal of any particulates and then through an electric heater. Flow rate is controlled by an automatic control valve and measured by a series of two rotameters. Water temperature measurements are made with a K-type thermocouple located upstream of the PHE. The water temperature is maintained within ±0.5 °C of the desired value, and pH is controlled within ±0.05 units of the set value. The pH electrode is standardized before each experiment (and occasionally during the tests) with standard buffer solutions at pH 7.0 and pH 9.0 at 25 or 40 °C. The particulate suspension (i.e. commercial particles in distilled water adjusted to a pH of about 8) is stirred continuously and introduced into the flow line via a FMI metering pump.

The test PHE (Model V2, VICARB) consists of eight plates and the supersaturated water passes through three flow channels. The characteristics of the PHE are summarized in Table 1. For most runs the direction of flow inside the PHE was upwards, although a few runs were carried out with the liquid flowing downwards, as recommended by the manufacturer for cases involving

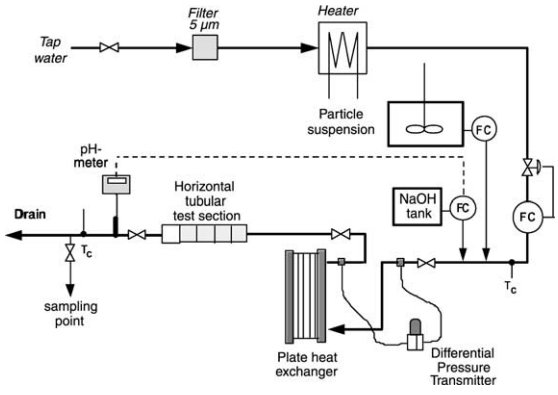

Fig. 1. Schematic diagram of the experimental test facility.

Table 1
Characteristics of the PHE (VICARB, V2)

Corrugation type	Chevron
Plate material	AISI 316
Plate thickness, s	0.6 mm
Corrugation angle, ϕ	60°
Corrugation pitch, d	8.2 mm
Plate height, d_p	2.92 mm
Plate width, w	76 mm
Flow section area	186 cm^2

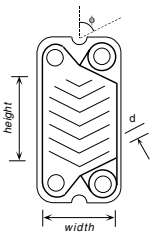

particulate suspensions. Downstream of the PHE a tubular test section is connected, so that the mass deposited (on appropriate semi-annular stainless steel coupons) can be measured at certain time intervals and compared with available precipitation fouling data from the same test section. Special 10×12 mm^2 rectangular coupons are used for the scanning electron microscope examination of the deposits.

The tap water used in the experiments contains approximately 82 mg/l Ca, 20 mg/l Mg and 360 mg/l HCO_3^-. Its chemical composition remains almost unchanged over the past several years. A detailed description of "pure" precipitation fouling experiments with a tubular test section and a complete analysis of the water can be found in [6].

Three types of commercial particles were used: two types of calcium carbonate having different characteristics (Solvay 90A and CARLO ERBA) and TiO_2 (Thon et Mulhouse, AT1). The particles were characterised by powder X-ray diffraction (Siemens, D500), scanning electron microscopy (JEOL, 6300) and inductively coupled plasma spectroscopy (Plasma 40, Perkin-Elmer). The specific surface area of the particles was determined by the BET method (Quantachrome). The size distribution of the particles suspended in distilled water at pH$\sim$8.5 was measured by a laser diffraction technique (Mastersizer X, Malvern). The morphology of the particles is shown in the micrographs of Fig. 2. Particle characteristics are summarised in Table 2. The aragonite particles contain about 0.2% w/w magnesium and seem to be agglomerates of elongated elementary crystallites (rod-like) with lengths of order 1 μm and diameter roughly 200 nm. The CARLO ERBA particles consist of rhombohedral crystals with sides in the range 1–10 μm (Fig. 2b) forming larger clusters (typical size 5–50 μm). The TiO_2 particles (Fig. 2c) seem to be agglomerates of tiny, fairly uniform (50–200 nm), elementary crystallites. With regard to specific surface area, the aragonite and TiO_2 particles have almost identical values, whereas the specific surface area of the calcite particles is an order of magnitude lower. The aragonite and the TiO_2 particles have been used in several particulate fouling studies [25,26].

The progress of the fouling process was monitored by measuring the increase of the pressure difference across the PHE using two differential pressure transmitters (DPX Fisher & Porter). The tests were conducted in the Reynolds number range between 500 and 2500. Reynolds number in a PHE is defined as $Re = V\rho d_h/\mu$, where V is the mean channel flow velocity, ρ the solution density, d_h the plate hydraulic diameter ($=2\,b$) and μ the liquid viscosity. In a PHE, V is defined as $V = q/nwb$, where q the liquid flow rate, n the number of flow channels, b the plate gap (plate height minus plate thickness) and w the plate width. At the end of each experiment the plates were opened and occasionally photographed, while the mass of the dry deposits on each plate was measured and collected for XRD analysis. Visual observations were made regarding the pattern and adhesion characteristics of the deposits. The same set of plates was used for about 20 runs before replacement with a new set.

It has been suggested [27] that air injection and the creation of two-phase flow inside the PHE for a certain period of time could increase the removal rate thus mitigating scaling. This suggestion was tested in this work with combined particulate/precipitation $CaCO_3$ deposits. Air was injected into the liquid line well upstream the entry to the PHE for a desired time period. Any deposit reduction could cause a decrease in the pressure drop in the PHE.

Finally, a series of "seeded" growth experiments were carried out to investigate the role of particles dispersed in a supersaturated solution on inducing bulk precipitation. These experiments were conducted in a three-necked flask, immersed in a temperature-controlled water bath. A tap water volume of 0.2 dm^3 (filtered through a 0.45 mm polycarbonate Nucleopore membrane) was used at 25 and 40 °C. The solution pH, adjusted to the desired value by dropwise addition of NaOH, was continuously monitored prior to particle addition and for the duration of the experiment, using a

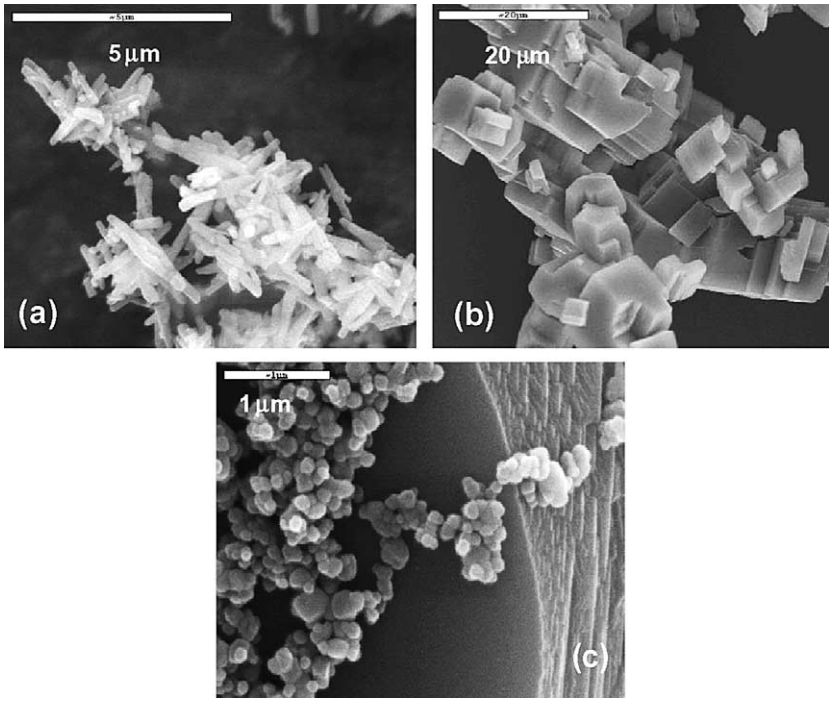

Fig. 2. SEM micrographs of commercial particles used in the experiments: (a) aragonite particles, (b) large calcite particles and (c) TiO_2 particles on top of a calcite crystal.

Table 2
Characteristics of the tested particles

Type	Crystalline phase	Particle size, $D(v, 0.5)$ (μm)	Specific surface area (m^2/g)	ζ-potential (mV)
$CaCO_3$, Solvay 90A	Aragonite	5.3	12.5	−26 (pH = 9) [25]
$CaCO_3$, Carlo Erba	Calcite	15	1.1 ± 0.2	Not available
TiO_2	Anatase	0.8	11.4	−50 (pH = 7) [26]

Metrohm 632-pH meter. The 10-ml suspension of particles was introduced to the solution dropwise at the desired particle concentration under continuous mild magnetic stirring.

4. Results and discussion

All the experiments (wall crystallization and bulk precipitation) were conducted at two temperatures, 25 and 40 °C; several particle concentrations and flow velocities were examined, especially with the aragonite particles. The pH was one of the main parameters investigated in this work and varied between 8 and 9.

The thermodynamic driving force for calcium carbonate crystallization either in the bulk or at the pipe wall (scale formation), is defined as the difference of Gibbs free energy between the supersaturated state and equilibrium:

$$\Delta G = -RT \ln \left[\frac{(Ca^{2+})(CO_3^{2-})}{K_{sp}} \right]^{1/2} \quad (1)$$

Here R is the gas constant, T is the absolute temperature and K_{sp} is the thermodynamic solubility product of the dominant polymorph. Quantities in parentheses denote activities of the corresponding ions. The term in brackets is the supersaturation ratio of the crystalline precipitate, defined as

$$S = \left[\frac{(Ca^{2+})(CO_3^{2-})}{K_{sp}} \right]^{1/2} \quad (2)$$

The solution speciation and the supersaturation ratios were calculated by the HYDRAQL computer code [28].

In supersaturated calcium carbonate solutions a number of polymorphs may be formed, including calcite, aragonite, vaterite and calcium carbonate monohydrate [3]. Calcite is the most stable and least soluble polymorph forming usually hard and tenacious scales [3,4]. Supersaturation in this work is computed with respect to calcite, which is found to be the predominant crystalline deposit for temperatures below 35 °C. As previously discussed, with the tap water used in this laboratory only the first two polymorphs have been identified in deposits. Vaterite has also been observed in deposits from synthetic waters [7]. A brief section describing the results of bulk precipitation studies precedes the main section with the results from the combined wall-crystallization experiments.

4.1. Bulk precipitation studies

A series of "seeded" growth experiments was carried out to investigate the effect of particle addition to water supersaturated with respect to $CaCO_3$ and the possible correlation of spontaneous bulk precipitation with wall crystallisation. In the pH range between 8 and 8.8 no spontaneous precipitation was observed (at least for a 2-h period) without particle addition, as indicated by the constant pH value of the solution.

Typical results from bulk precipitation experiments are shown in Fig. 3. For a pH of 8.7 at 25 °C ($S = 6.0$) the "blank" experiment (i.e. no particle addition) displays only a slight increase in pH over 1 h. Upon introduction of the fine aragonite particles at $C_p \geqslant 10$ mg/l into the supersaturated solution, precipitation starts immediately, accompanied by reduction in the solution pH. In accord with many studies on seeded crystal growth [20–22], an increase of the added particles leads to a larger precipitation rate. This behaviour is well documented in the literature, where in general the precipitation rate increases with seed concentration, but if the rate constant is expressed per unit mass of seeds the rates are comparable [21,22]. On the other hand, a 40-mg/l concentration of calcite particles does not appear to induce precipitation, at least for the duration of the experiment. A 10-fold increase, however, of added calcite results in a precipitation behaviour similar to that for the 40 mg/l aragonite particle concentration. Since the specific surface area of the large calcite particles is about ten times lower than the surface area of the aragonite particles, it seems that if the rate constants for the two types of $CaCO_3$ particles are expressed per unit surface area of the added particles, the rates are similar. A totally different picture is obtained with the dissimilar in nature TiO_2 particles; even at a concentration as high as 200 mg/l these particles do not appear to affect bulk precipitation characteristics. Regarding the experiments at 40 °C, a similar picture is obtained for the bulk precipitation, if the results are expressed for the same supersaturation ratio.

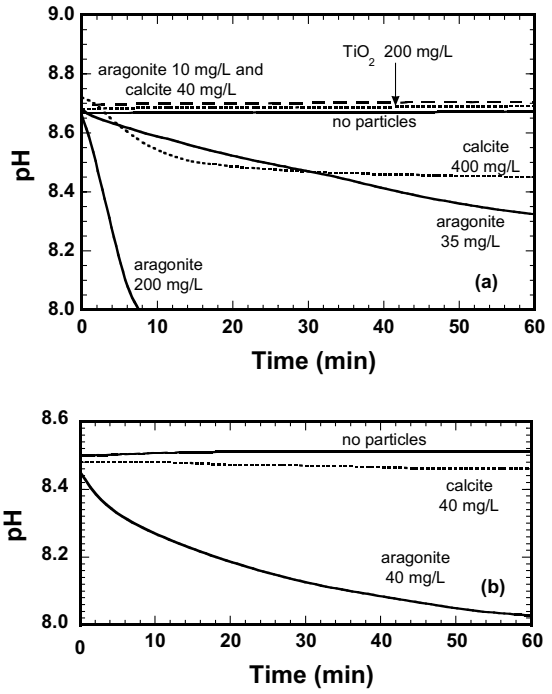

Fig. 3. pH temporal change of supersaturated $CaCO_3$ solutions in the presence and absence of particles at $S \sim 6$: (a) $T = 25$ °C and (b) $T = 40$ °C.

The precipitates in the presence or absence of added particles, as assayed by X-ray diffraction and observed under a scanning electron microscope, are in most cases mixed calcite and aragonite crystals. However, aragonite seed crystals seem to promote the formation of mostly aragonite precipitates, whereas calcite seeds favour calcite crystal formation.

4.2. Scaling experiments in the presence of particles

Initially, experiments were carried out under pure crystallisation conditions; i.e without particle addition. The deposition pattern is found to be similar to that observed in a pipe flow [7]; i.e. the deposit layer appears to be rather uniform over the entire plate, with the exception of the region downstream (behind) the contact points, where reduced deposits are observed. Most of the results in this investigation are presented in terms of the temporal variation of the relative pressure drop in the PHE due to deposition, DP/DP_i, where DP_i is the initial pressure drop with no scale. The pressure drop increase in the PHE follows the increase in the deposited mass (measured in the horizontal tubular test section) as illustrated in Fig. 4 for a pure precipitation experiment; however, for relatively thick layers (>0.3 mm) the rate of

pressure drop increase is greater than that of deposited mass, because of the severe blocking of the PHE flow passages. Furthermore, the deposited mass in the vertical plates in the presence or absence of particles is correlated quite well with the deposited mass in the horizontal tubular test section, as shown in Fig. 5. In the present experiments no observable maldistribution in the three PHE channels was observed, as deduced from the almost identical amount of deposits weighed in all six plates after each run. In PHEs with a large number of plates (>20), maldistribution is almost always observed, emanating from the difference between the pressure profiles in the inlet and outlet ports [25].

The presence of fine aragonite particles exerts a great influence on almost all deposition characteristics compared to those of "pure" precipitation deposits. A typical case is illustrated in Fig. 6 for a low supersaturation ratio ($S \approx 5$) for which no visible or measurable deposition occurs in the absence of particles, for a period of at least 5 h. However, aragonite particle addition causes a rather sharp increase of pressure drop, resulting from the build-up of deposits in the PHE. This pressure drop variation is drastically different than the nearly constant DP obtained under the same conditions in the absence of particles. The presence of particles tends to induce and to accelerate the precipitation process at short times. A significant increase in the pressure drop and accumulated deposits due to the aragonite particle addition occur for all supersaturations tested, as shown in Fig. 7, for an intermediate supersaturation ratio ($S \approx 8$).

The effect of large calcite particles (similar in nature to the precipitating system) and of fine TiO_2 particles (dissimilar) is also illustrated in Figs. 6 and 7. Contrary to the observed dramatic effect of the aragonite particles, the use of the calcite particles does not appear to result in noticeable deposit enhancement. The small effect of

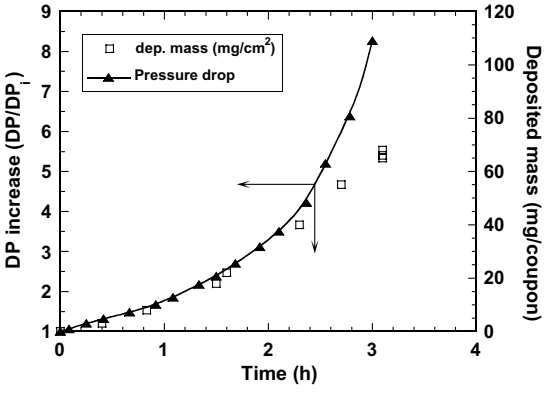

Fig. 4. Correlation between the pressure drop inside the PHE and the mass of deposits in the horizontal pipe section, in the absence of particles. Experimental conditions: $V = 0.17$ m/s, $T = 39$ °C, pH = 9.05 ($S = 9.5$).

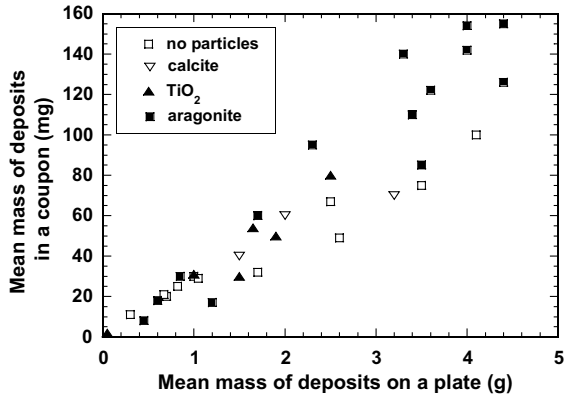

Fig. 5. Correlation between the mean mass of deposits on the plates and that on the semi-annular coupons, under the same conditions.

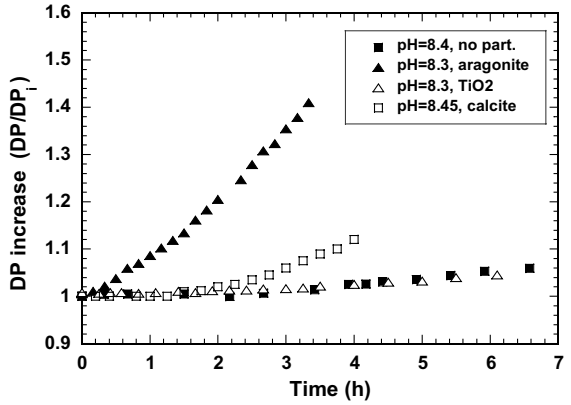

Fig. 6. Influence of the presence of particles on deposit formation at relatively low supersaturation, $S \sim 5$ ($T = 40$ °C, $V = 0.17$ m/s, $C_p = 35$–45 mg/l).

calcite particles depicted in Fig. 7 is attributed to the smaller pH value of the combined run. The negligible or small effect of the relatively large calcite particles on the deposition process is apparently related to their low specific area and, consequently, their low "seeding" effect. It will be recalled that with regard to the specific area, 40 mg of aragonite particles correspond roughly to 500 mg of calcite particles. On the other hand, the specific area of the TiO_2 particles is almost identical to that of the aragonite seeds; thus, the different influence they exert on scaling is apparently due to their different surface characteristics.

The results at 40 °C are summarized in Fig. 8, where the pressure drop increase, measured 3-h after the start of each run, is plotted against the supersaturation ratio. There is a systematic DP increase in the presence of the

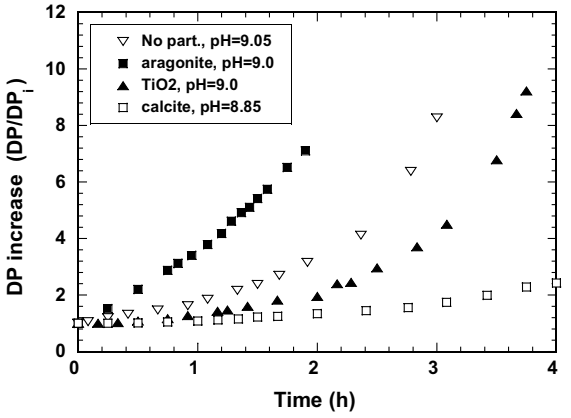

Fig. 7. Influence of the presence of particles on deposit formation at intermediate supersaturation ratios, $S \sim 8$ ($T = 40$ °C, $V_{plate} = 0.17$ m/s, $C_p = 35$–40 mg/l).

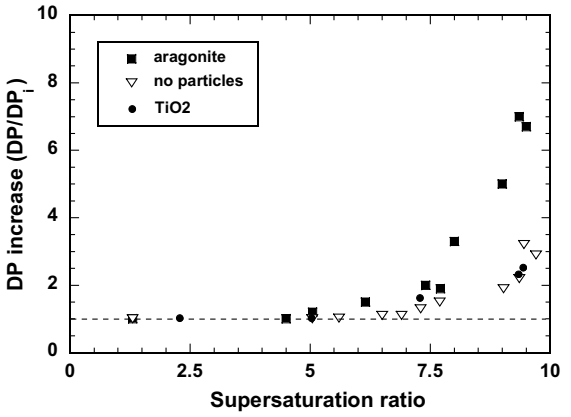

Fig. 8. Pressure drop increase in the presence of particles at various supersaturation levels (Run time = 3 h, $T = 40$ °C, $V_{plate} = 0.17$ m/s, $C_p = 35$–40 mg/l).

aragonite particles; furthermore, in the absence of particles, incipient deposition occurs at $S \sim 7$, whereas addition of aragonite particles shifts the onset of the process at $S \sim 5$.

On a qualitative basis, the trends are similar between bulk precipitation and wall crystallisation in the presence of particles, although some minor differences are observed. For example, both processes are intensified with increasing particle concentration, C_p; however, while $C_p = 10$ mg/l of aragonite particles at pH 8.7 does not affect the bulk precipitation process (as shown in Fig. 3), the same concentration causes a significant increase in the deposited mass. Another difference is related to the polymorphism of the precipitates and the deposits, discussed in Section 4.3.

4.3. Characterisation and morphology of deposits

4.3.1. Aragonite particles

An interesting feature of the increased deposits caused by addition of aragonite particles is their "rippled" appearance (ridges rising above a relatively uniform base layer), illustrated in the pictures of Fig. 9. A schematic representation of these ripples is depicted in Fig. 10. The "ripples" form just behind the contact points of the corrugated plates and extend into the plate "valley" covering a small triangular area. It is evident that the rippled deposits are aligned transversely to the "zig–zag" flow direction of the liquid inside the plate channel. The orientation of the ripples, which is *normal* to the local flow direction, is also evident at the inlet and outlet of each plate (Fig. 9). In regions of low liquid velocity (around the two corners and at the sides of the plate) more deposits are formed; it will be recalled that no such observations are made in "pure" precipitation runs, where a rather uniform layer is obtained.

The alignment of the ridges in a direction transverse to the main flow is clear in the horizontal tubular test section, as shown in the pictures of Fig. 11 for two flow velocities. Under certain conditions, the ripples cover the whole pipe circumference, as discussed in [16]. These rippled deposits first appear at the bottom of the horizontal tube, while a base layer of relatively hard scale forms uniformly around the tube circumference. With time the rippled deposits extend and cover the entire circumference. The deposits in the ridges, both in the plates and in the tubular test section, can be easily removed when they are dry, uncovering a uniform layer of hard scale (right on the surface), familiar from runs with no particles. The mass of these hard deposits compares well with crystallization-only results under the same conditions.

The ease of removing the rippled deposits does not imply that they are "fluffy", since they cannot be removed by simple water rinsing. Furthermore, a run was made to test the suggestion [27] that air injection for a certain period of time could increase the removal rate thus mitigating scaling. In that test no reduction of pressure drop was noticed after injecting air simultaneously with the liquid for a period of 15 min at the end of a combined run, as opposed to experiments with the $CaSO_4$ system where noticeable reduction in pressure drop was reported [28] after the injection of air. The explanation of the different behaviour of the two scaling systems may lie in the different mechanism of deposition. The dominant mechanism in $CaSO_4$ scale formation seems to be particulate deposition [14]. The $CaSO_4$ scale layers are not as compact and coherent as the $CaCO_3$ layers and this may explain the asymptotic fouling obtained with $CaSO_4$ as well as the substantial deposit removal by air injection. On the other hand, even the combined particulate/precipitation $CaCO_3$ deposits

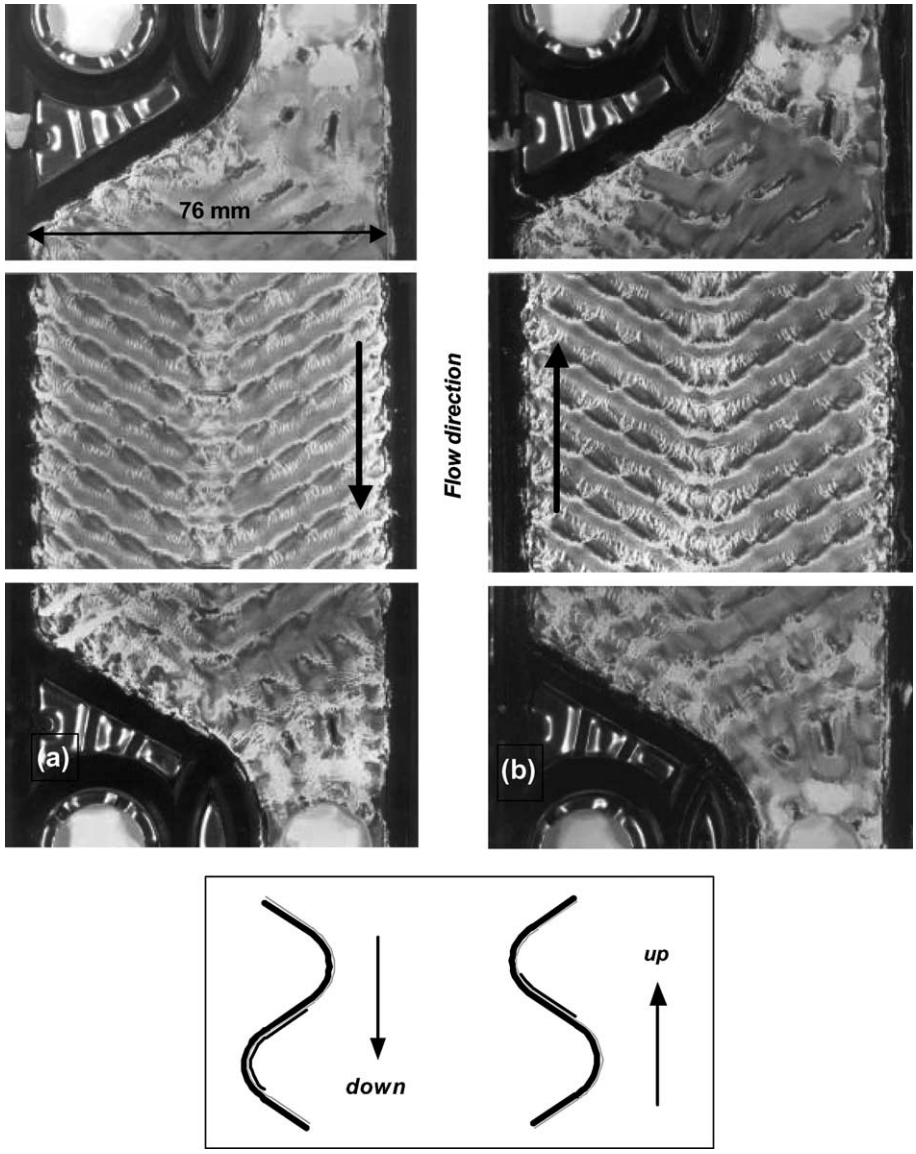

Fig. 9. Pictures of plates with "combined" deposits resulting from the addition of aragonite particles. Conditions: (a) downflow, $V = 0.17$ m/s, $C_p = 36$ mg/l, $T = 25$ °C, pH = 8.9 ($S = 7.5$), time = 3.2 h; (b) upflow, $V = 0.17$ m/s, $C_p = 38$ mg/l, $T = 25$ °C, pH = 8.85 ($S = 7.4$), time = 4 h.

appear to be fairly coherent and increased flow shear stress may not be capable of removing part of the deposits.

Fig. 12 illustrates SEM micrographs showing different aspects of the rippled deposits formed at 25 °C. The ripples are not very regular and a chain-like ridge is usually observed (Fig. 12a). A side view of a ridge (Fig. 12b) and a magnified view (Fig. 12c) reveal that the ridges also consist of agglomerates of calcite crystals, having a size smaller than those comprising the base film in the "valley" (Fig. 12d). Occasionally, aragonite clusters are observed in the deposits, similar in morphology with the added particles.

The main polymorphic phase of the deposits formed at 25 °C in the presence of aragonite particles is calcite as identified from XRD analysis and seen in the SEM pictures. This observation suggests that the increased mass deposited in the "combined" runs is not due to a greatly increased particulate deposition (although some increase may occur), but rather to an enhancement of the wall crystallisation rate induced by the presence of particles.

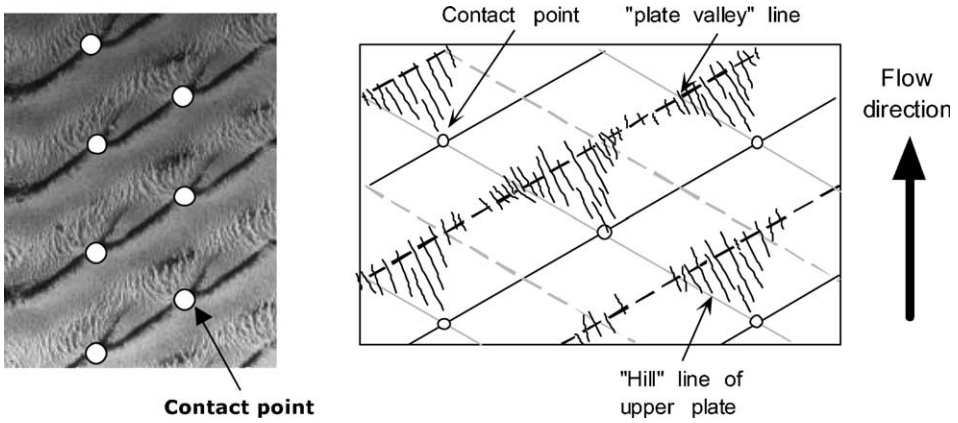

Fig. 10. Picture and schematic representation of rippled deposits behind the contact points of corrugated plates.

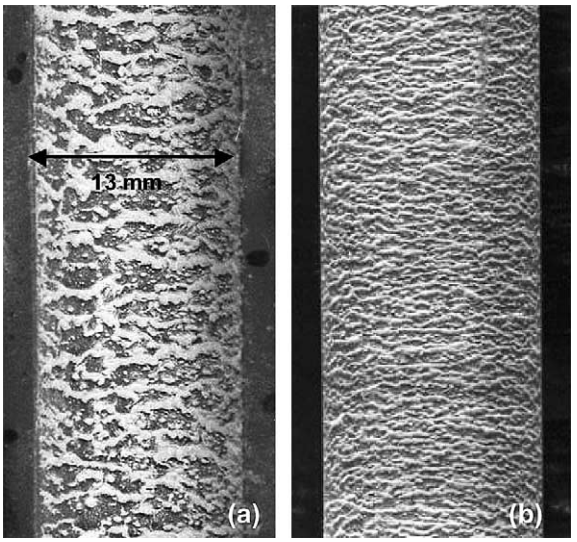

Fig. 11. Pictures of semi-annular coupons with "combined" deposits resulting from the addition of aragonite particles. Conditions: $C_p = 36$ mg/l, $T = 25$ °C, pH = 8.9 ($S = 7.5$). (a) $V = 0.65$ m/s, time = 3.1 h and (b) $V = 1.3$ m/s, contact time = 2.3 h. The deposited mass on both coupons is identical, 155 mg.

4.3.2. Calcite and TiO_2 particles

Pictures and micrographs of deposits formed in the presence of large calcite and TiO_2 particles are presented in Figs. 13 and 14, respectively. The pictures in Fig. 13 are almost identical with the corresponding pictures of deposits from "pure" precipitation runs. In the presence of the large calcite particles the dominant polymorph at 40 °C is calcite as evidenced from SEM micrographs and XRD analysis, in contrast with the mixed aragonite/calcite deposits obtained with no particles. A comparison of the XRD traces of various deposits formed at 40 °C with and without addition of particles is shown in Fig. 15. The traces corresponding to deposits with no added particles and to deposits with the presence of aragonite particles show that they consist of both calcite and aragonite. On the other hand, the presence of TiO_2 particles and, most notably, of calcite particles, suppresses the aragonite formation.

As illustrated in Figs. 6 and 7, the presence of TiO_2 particles does not affect the deposited mass of $CaCO_3$. Furthermore, the deposition of TiO_2 particles themselves (in "pure" particulate runs) does not seem to contribute to a measurable degree. Only a scanty mass of TiO_2 deposits can be measured on the plates in runs at $S \sim 1.5$ (no scaling tendency) for the same particle concentration as in the combined experiments (Fig. 14c). In the latter, the TiO_2 particles simply deposit on the substrate and on top and side faces of the calcite crystals (Fig. 12a and b). The presence of the TiO_2 particles causes three rather minor changes in the deposit characteristics. (i) The deposits with particles appear to be somewhat less coherent than those obtained in "pure" precipitation runs. (ii) The calcite particles in the deposits appear to be somewhat distorted (more rounded) with more macro steps. (iii) Even at 40 °C calcite remains the dominant polymorph of the deposits. An interesting point in the TiO_2 combined deposits is the significant mass of TiO_2 particles entrapped in the calcium carbonate deposits, in agreement with the finding of McGarvey and Turner [18]. Chemical analysis of these deposits showed that the contribution of TiO_2 particles in the combined deposits may reach 7% of the total deposit mass on a weight basis. This finding is also supported by the relatively high concentration of TiO_2 particles seen in the micrographs of Fig. 12. When compared with the deposits formed in "pure" particulate runs, the TiO_2 mass in the combined runs increases by a factor as large as 100. Part of this increase may be attributed to the increased surface area provided by the calcite crystals and another part to the

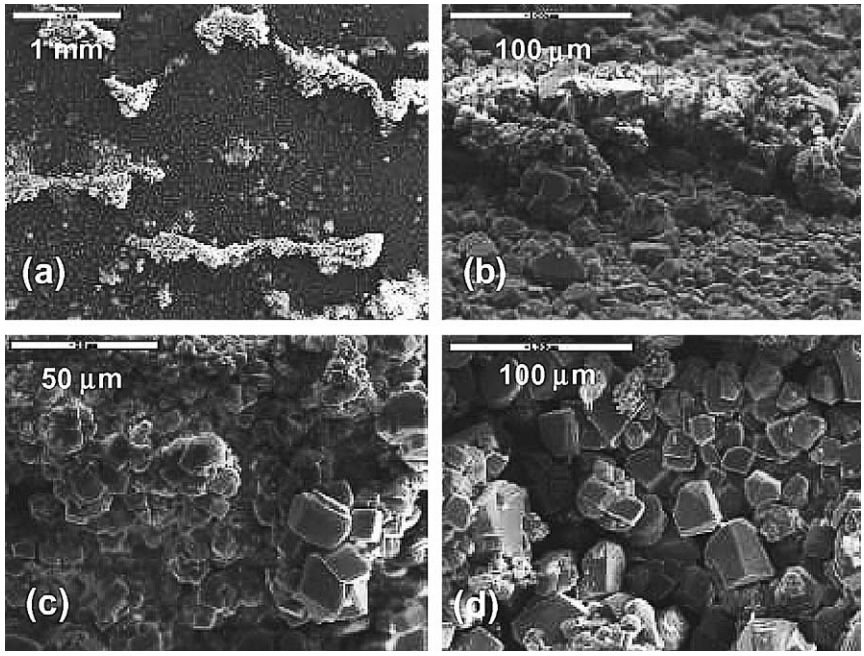

Fig. 12. Micrographs of "combined" deposits resulting from the addition of aragonite particles: (a) rippled deposits, (b) deposits as seen after tilting the SEM stage by 60°, (c) deposits on a "ridge" and (d) deposits in a "valley". Conditions: $C_p = 36$ mg/l, $T = 25$ °C, pH = 8.9 ($S = 7.5$), $V_{\text{plate}} = 0.17$ m/s.

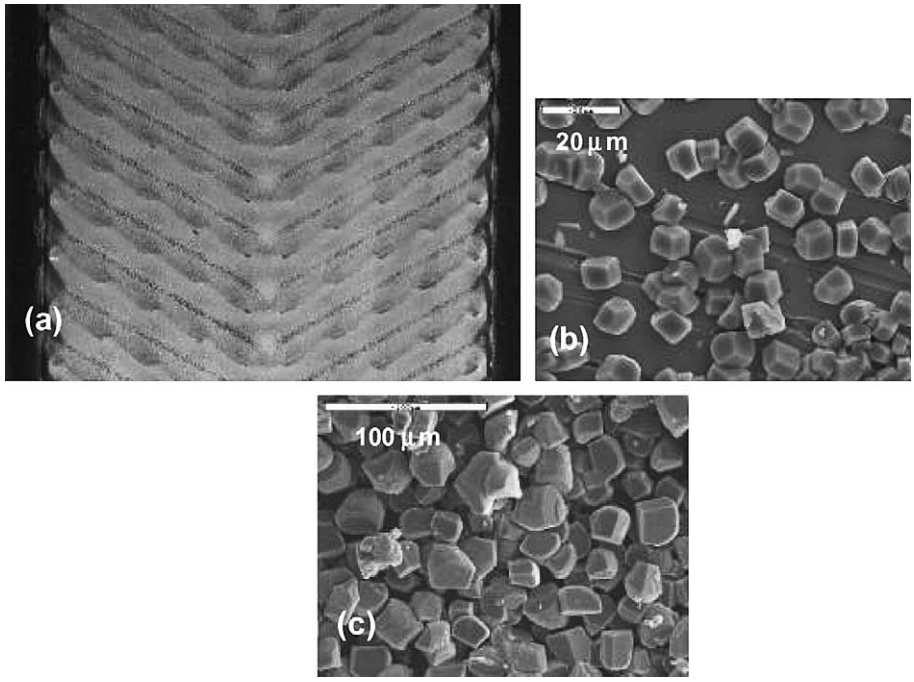

Fig. 13. (a) Picture of deposits formed in the presence of large calcite particles (contact time 4h); (b) and (c) micrographs of deposits at contact time 1 h and 4 h, respectively. Conditions: $C_p = 30$ mg/l, $T = 25$ °C, pH = 8.9 ($S = 7.5$), $V_{\text{plate}} = 0.17$ m/s.

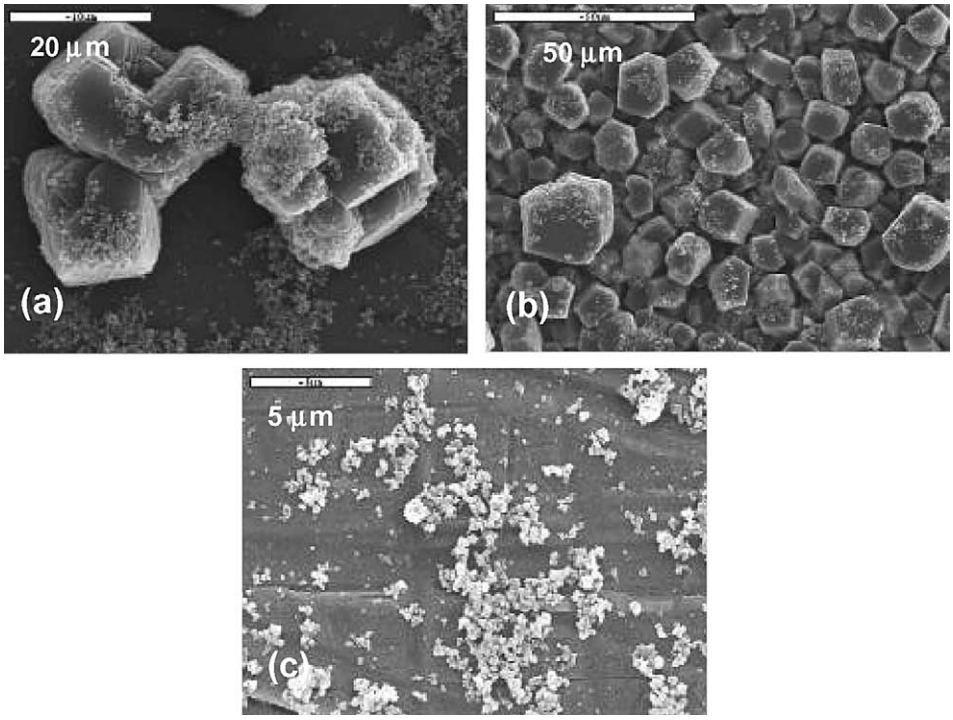

Fig. 14. Micrographs of 'combined' deposits in the presence of TiO_2 particles. Conditions: $C_p \sim 40$ mg/l, $T = 40$ °C, $V_{plate} = 0.17$ m/s: (a) pH = 8.35, (b) pH = 8.9 and (c) pH = 7.5 (pure particulate run).

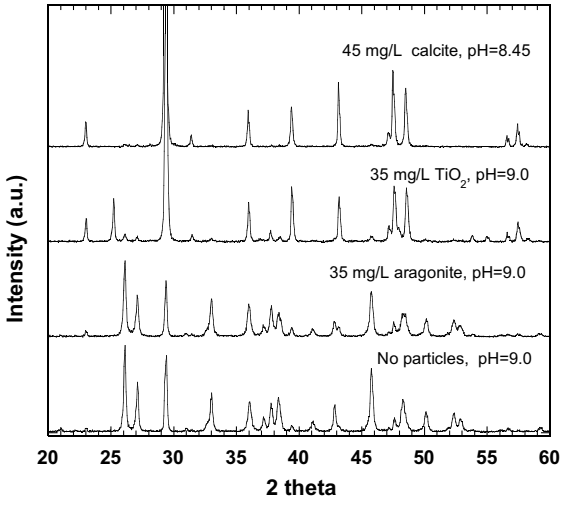

Fig. 15. X-ray powder diffraction spectra of deposits formed at 40 °C in the presence or absence of particles.

cementation of these particles to the calcite crystals before their resuspension.

4.4. Influence of particle concentration

The effect of added aragonite particle concentration (C_p) on scale formation at constant flow velocity, supersaturation ratio and temperature is shown in Fig. 16 for five particle concentrations, namely 0, 5, 10, 40 and 100 mg/l. In general, an increase of C_p tends to increase the relative enhancement of scale formation as evidenced from the increased pressure drop and the increased accumulation of deposits on the plates, in agreement with similar studies in the literature. Even at the lowest particle concentration tested (5 mg/l), an increased deposition rate is observed. At this particle concentration, the regions with rippled deposits are fewer, the length of the ridges is smaller and their wavelength is larger when compared with the case of $C_p \sim 40$ mg/l.

4.5. Influence of flow velocity

Flow velocity is an important factor on scale formation. It was recognized very early that velocity affects the fouling process as regards both deposition and removal steps [2,10] and that, in general, high velocities may reduce scale formation (due to increased detachment), something that is true especially for particulate fouling. However, in cases where pure $CaCO_3$ precipitation fouling occurs, high flow velocity results in higher deposition rates and more compact scale layers [7,29], since the deposition process is controlled by mass transfer. When pure $CaCO_3$ precipitation occurs, a compact and tenacious scale layer forms in most cases and the removal rate seems to be insignificant. The effect

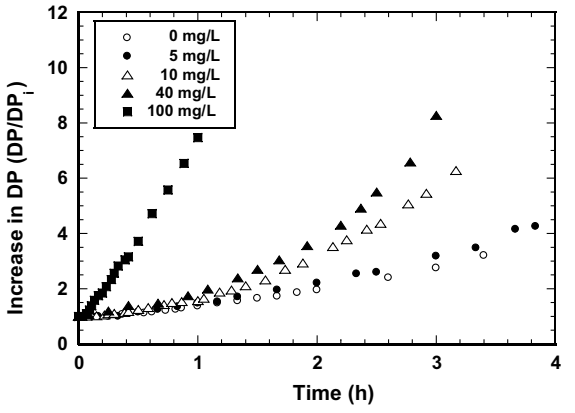

Fig. 16. Influence of the concentration of added aragonite particles on the temporal change of pressure drop in the PHE ($T = 25$ °C, $V_{plate} = 0.17$ m/s, pH~8.9).

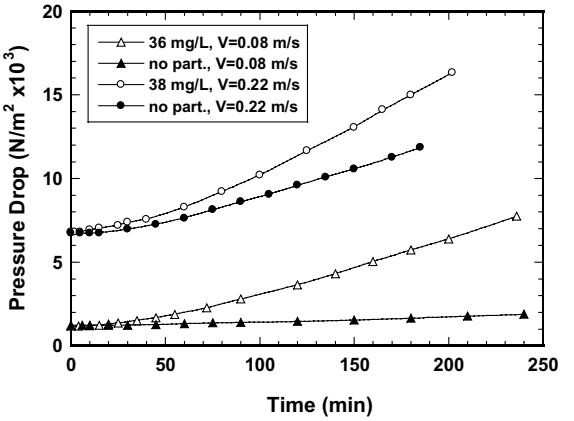

Fig. 17. Temporal change of pressure drop inside the PHE for two different flow rates in the presence and absence of aragonite particles ($T = 25$ °C, pH = 8.9–9.0, $C_p = 35$–40 mg/l).

of velocity on removal depends primarily on the wall shear stress and the mechanical strength of the scale layer.

Fig. 17 illustrates the increase of pressure drop inside the PHE for two different flow rates in the presence and absence of aragonite particles; all other experimental conditions are identical. It is clear that the deviation between the runs in the presence and in the absence of particles is smaller at the higher flow velocity. This trend with increasing flow rate is better depicted in Fig. 18, where the pressure drop increase at the end of a 3-h period is plotted as a function of flow rate in the presence and absence of particles. The relative pressure drop increase in the presence of aragonite particles tends to decrease substantially with increasing flow velocity, approaching the relative increase of runs without particles or in the presence of calcite and TiO_2 particles. This trend may be attributed to the increasing removal rate of deposited particles with flow velocity, which implies that a particulate process is also operative in the formation of the rippled deposits.

Although a velocity increase does not change the general macroscopic appearance of the rippled deposits, it is noted that at higher velocities the deposits tend to be more compact and are removed with greater difficulty than those formed at lower velocities. The increasing compactness of the deposits with the flow velocity has been also observed in studies in the absence of particles, but further compactness may result from a lower degree of aragonite particle incorporation in the crystalline deposit layer. Another characteristic of increasing the flow velocity is that the mean "wavelength" of the rippled deposits decreases (as also seen in the tubular coupons of Fig. 11). There is also a tendency for ripple formation at the troughs of the corrugated plate.

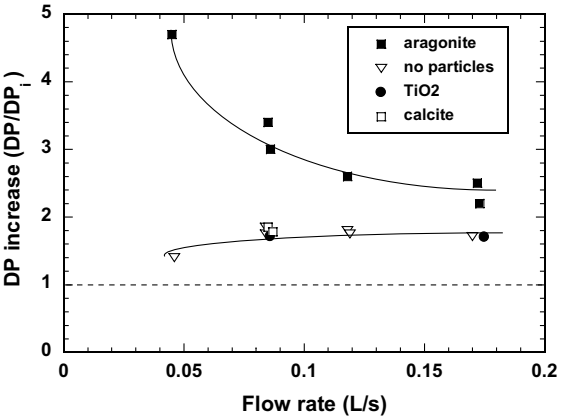

Fig. 18. Effect of flow rate on pressure drop increase at the end of a 3-h period ($T = 25$ °C, pH = 8.9–9.0, $C_p = 35$–40 mg/l).

4.6. Influence of flow direction in the PHE

A limited number of runs were made with the flow direction downwards (as is recommended for flows containing particulate matter in PHE) in order to assess the effect of gravity on the enhanced scale formation. No difference was noticed regarding scale build-up and, even the morphology and general appearance of the deposits are similar as illustrated in Fig. 6. The formation of rippled deposits on the downward side of a plate pitch may lead to the tentative conclusion that gravity does not play a major role in the formation of these ripples.

5. Concluding remarks

The effect of added particulate matter on $CaCO_3$ scale formation has been investigated for three different

types of particles. The duration of the experiments did not exceed five hours and, obviously, the present results cannot be extrapolated for long-term operating conditions. The presence of a low concentration of fine aragonite particles not only has a synergistic role (significantly augmenting the deposited mass), but also induces the onset of scaling at relatively lower supersaturation values, for which no precipitation fouling is otherwise observed. The enhancement of scale formation appears to be independent of the flow direction inside the PHE compartments and it tends to be reduced with increasing flow velocity. The mechanism of this enhancement by aragonite particles is not obvious at this time, but it may be related to an increased mass transfer rate due to microroughness caused by the deposition and cementation with $CaCO_3$ of the dispersed aragonite clusters. In addition, and especially at low supersaturation conditions, the aragonite particles may act as nuclei on which precipitation occurs. The subsequent formation of rippled deposits seems to further accelerate the deposition rate. The deposit enhancement is larger at low flow velocities; an increased detachment rate with increasing flow velocity may remove part of the initially deposited particles reducing the net effect of synergism between particulate and precipitation deposition. In contrast, the addition of small TiO_2 particles and of relatively large calcite crystals in concentrations up to 100 mg/l does not cause an appreciable increase in scale formation; however, these particles tend to reduce somewhat the deposit strength and to affect the deposit morphology. The negligible effect of relatively large calcite particles (compatible with the precipitating species) may be attributed to their low specific surface area. Finally, bulk precipitation experiments can serve as a rough guide for assessing the effect of added particles on a precipitating system. More work is certainly required in order to clarify these complicated phenomena.

Acknowledgements

This work has been financially supported by the Commission of European Communities (JOULE Programme) under Contract JOE3-CT97-0053. The authors wish also to thank Mr. V. Hadjiapostolou for assistance in the experimental work, the Analytical Laboratory of CPERI for the XRD spectra and the SEM pictures and Mr. V. Kalaitzidis for the pictures of scaled plates.

References

[1] T.R. Bott, Fouling of Heat Exchangers, Elsevier Science, Amsterdam, 1995.
[2] N. Epstein, Thinking about heat transfer fouling: a 5×5 matrix, Heat Transfer Eng. 4 (1983) 43–56.
[3] J.C. Cowan, D.J. Weintritt, Water-Formed Scale Deposits, Gulf Publ. Co, Houston, 1976.
[4] S.H. Lee, J.G. Knudsen, Scaling characteristics of cooling tower water, ASHRAE Trans. 85 (Part I) (1989) 281–302.
[5] A.P. Watkinson, Water quality effects on fouling from hard waters, in: J. Taborek et al. (Eds.), Heat Exchangers Theory and Practice, Hemisphere Publ. Co, Washington, 1983, pp. 853–861.
[6] N. Andritsos, M. Kontopoulou, A.J. Karabelas, P.G. Koutsoukos, $CaCO_3$ scale layers formed under isothermal flow conditions, Can. J. Chem. Eng. 74 (1996) 911–919.
[7] N. Andritsos, A.J. Karabelas, P.G. Koutsoukos, Morphology and structure of $CaCO_3$ deposit formation under isothermal conditions, Langmuir 13 (1997) 2873–2879.
[8] M. Reppich, Use of high performance plate heat exchangers in chemical and process industries, Int. J. Thermal Sci. 38 (1999) 999–1008.
[9] H. Müller-Steinhagen, J. Middis, Particulate fouling in plate heat exchangers, Heat Transfer Eng. 10 (1989) 30–36.
[10] J. Taborek, T. Aoki, R.B. Ritter, J.W. Palen, J.G. Knudsen, Predictive methods for fouling behavior, Chem. Eng. Progr. 68 (2) (1972) 59–67.
[11] R.W. Morse, J.G. Knudsen, Effect of alkalinity on the scaling of simulated cooling tower water, Can. J. Chem. Eng. 55 (1977) 272–278.
[12] D. Hasson, J. Zahavi, Mechanism of calcium sulfate scale deposition on heat-transfer surfaces, Ind. Eng. Chem. Fund. 9 (1970) 1–9.
[13] D. Bramson, D. Hasson, R. Semiat, The roles of gas bubbling, wall crystallization and particulate deposition in $CaSO_4$ scale formation, Desalination 100 (1995) 105–113.
[14] D. Hasson, Progress in precipitation fouling: a review, in: T.R. Bott et al. (Eds.), Understanding Heat Exchanger Fouling and its Mitigation, Begell House, New York, 1999, pp. 67–89.
[15] B. Bansal, H. Müller-Steinhagen, X.D. Chen, Effect of suspended particles on crystallization fouling in plate heat exchangers, J. Heat Transfer 119 (1997) 568–574.
[16] N. Andritsos, A.J. Karabelas, The Influence of particulates on $CaCO_3$ scale formation, J. Heat Transfer 121 (1999) 225–227.
[17] J.S. Gundmudsson, T.R. Bott, Deposition of silica from geothermal waters on heat transfer surfaces, Desalination 28 (1979) 125–145.
[18] G.B. McGarvey, C.W. Turner, Synergism models for heat exchanger fouling mitigation, in: T.R. Bott et al. (Eds.), Understanding Heat Exchanger Fouling and its Mitigation, Begell House, New York, 1999, pp. 155–161.
[19] R.L. Webb, W. Li, Fouling in enhanced tubes using cooling tower water, Int. J. Heat Mass Transfer 43 (2000) 3567–3578.
[20] M. Perrakis, N. Andritsos, A.J. Karabelas, $CaCO_3$ scaling under constant heat flux, in: T.R. Bott et al. (Eds.), Understanding Heat Exchanger Fouling and its Mitigation, Begell House, New York, 1999, pp. 185–192.
[21] G.H. Nancollas, M.M. Reddy, The crystallization of calcium carbonate II. Calcite growth mechanism, J. Colloid Interface Sci. 37 (1971) 824–830.
[22] M.M. Reddy, W.D. Gaillard, The crystallization of calcium carbonate II. Calcite growth mechanism, J. Colloid Interface Sci. 80 (1981) 171–178.

[23] T.G. Sabbides, P.G. Koutsoukos, The crystallization of calcium carbonate in artificial seawater; role of the substrate, J. Crystal Growth 133 (1993) 13–22.
[24] W.A. House, J.A. Tutton, An investigation of the heterogeneous nucleation of calcite, J. Crystal Growth 56 (1982) 699–710.
[25] B. Thonon, J.M. Grillot, R. Vidil, Liquid side fouling of plate heat exchangers, in: C.B. Panchal et al. (Eds.), Fouling Mitigation of Industrial Heat-Exchange Equipment, Begell House, New York, 1996, pp. 537–548.
[26] S. Grandgeorge, C. Jallut, B. Thonon, Particulate fouling of corrugated plate heat exchangers. Global kinetic and equilibrium studies, Chem. Eng. Sci. 53 (1998) 3051–3071.
[27] T. Kho, H.M. Zettler, H. Müller-Steinhagen, D. Hughes, Effect of flow distribution on scale formation in plate and frame heat exchangers, Trans. Inst. Chem. Eng. 75 (1997) 635–640.
[28] C. Papelis, K.F. Hayes, J.O. Leckie, HYDRAQL, Technical Report No. 306, Stanford, CA, Stanford University, 1988.
[29] D. Hasson, M. Karmon, Novel process for lining water mains by controlled calcite deposition, Corros. Prevent. Control 31 (1984) 9–17.